Journal of General Virology (2005), **86**, 2839–2848 DOI 10.1099/vir.0.81218-0

Location of, immunogenicity of and relationships between neutralization epitopes on the attachment protein (G) of *Hendra virus*

John R. White, Victoria Boyd, Gary S. Crameri, Christine J. Duch, Ryan K. van Laar,† Lin-Fa Wang and Bryan T. Eaton

CSIRO Division of Livestock Industries, Australian Animal Health Laboratory, Geelong, VIC 3220, Australia

Correspondence
John R. White
John.White@csiro.au

Epitopes involved in a protective immune response to *Hendra virus* (HeV) (*Henipavirus*, *Paramxyoviridae*) were investigated by generating five neutralizing monoclonal antibodies (mAbs) to the virus attachment protein (G) of HeV (HeV G) and sequencing of the G gene of groups of neutralization-escape variants selected with each mAb. Amino acid substitutions occurred at eight distinct sites on HeV G. Relationships between these sites were investigated in binding and neutralization assays using heterologous combinations of variants and mAbs. The sites were also mapped to a proposed structural model for the attachment proteins of *Paramyxoviridae*. Their specific locations and the nature of their interactions with the mAb panel provided the first functional evidence that HeV G in fact resembled the proposed structure. Four sites (aa 183–185, 417, 447 and 570) contributed to a major discontinuous epitope, on the base of the globular head, that was similar to immunodominant virus neutralization sites found in other paramyxoviruses. Amino acid similarity between HeV and *Nipah virus* was relatively highly conserved at these sites but decreased significantly at the other sites identified in this study. These included another discontinuous epitope on the base of the head region defined by sites aa 289 and 324 and well separated epitopes on the top of the head at sites aa 191–195 and 385–356. The latter epitope corresponded to immunodominant neutralization sites found in *Rinderpest virus* and *Measles virus*.

Received 30 May 2005
Accepted 11 July 2005

INTRODUCTION

Hendra virus (HeV) and *Nipah virus* (NiV) cause respiratory and encephalitic disease syndromes in humans and other mammals (Murray *et al.*, 1995; Middleton *et al.*, 2002; Chua, 2003). Both viruses possess negative-sense RNA genomes, genetic organization strategies and protein structures that lead to their classification in a newly defined genus, *Henipavirus*, within the subfamily *Paramyxovirinae* (family *Paramyxoviridae*) (Wang *et al.*, 1998, 2000, 2001). *Hendra virus* was first isolated from fatal infections of horses and a human in Queensland in 1994 (Selvey *et al.*, 1995; Murray *et al.*, 1995). Subsequent equine isolations were made in 1995 (also involving another human fatality) (Rogers *et al.*, 1996), in 1999 (Field *et al.*, 2000) and from a single case near Townsville, Queensland, as reported by local veterinary authorities in 2004 (Anonymous, 2004). *Nipah virus* first manifested in 1998 as the agent responsible for an extensive disease outbreak in Malaysian pigs, which was spread to humans and caused the death of 105 people (Chua *et al.*, 1999; Mohd Nor *et al.*, 2000; Chua *et al.*, 2000; Wang *et al.*, 2001; AbuBakar *et al.*, 2004). *Nipah virus* was also responsible for fatal disease outbreaks in humans in Bangladesh (Hsu *et al.*, 2004). The flying fox (*Pteropid* sp.) populations of Australia and South East Asia are a natural reservoir of henipaviruses (Young *et al.*, 1996; Halpin *et al.*, 2000; Johara *et al.*, 2001; Chua *et al.*, 2002).

HeV and NiV possess 83 % amino acid identity and extensive serological cross-reactivity (Chua *et al.*, 2000; Harcourt *et al.*, 2000; Wang *et al.*, 2001). Neither shows perceptible serological cross-reactivity with other *Paramyxoviridae* (Wang *et al.*, 2001). Cross-neutralization tests using polyclonal antisera have shown a consistent and reciprocal four to eightfold difference in titres between the viruses (Harcourt *et al.*, 2000). Additionally, Tamin *et al.* (2002) found that vaccinia virus-expressed NiV envelope glycoproteins induced neutralizing antibodies to both viruses, and a soluble form of the HeV attachment protein (HeV G) elicited a pronounced cross-reactive neutralizing antibody response to NiV (Bossart *et al.*, 2005). Therefore, we were interested in the nature and location of virus neutralization epitopes on HeV G and the extent of their

†Present address: The Peter MacCallum Cancer Centre, St Andrews Place, East Melbourne, VIC 3002, Australia.

conservation on NiV G. Characterization of henipavirus neutralization sites will assist studies of host cell tropism, the development of diagnostic assays and potentially provide reagents for vaccine development and validation.

The attachment proteins of members of the family *Paramyxoviridae* appear to possess a similar conformation (Colman *et al.*, 1993; Langedijk *et al.*, 1997; Pitt *et al.*, 2000; Vongpunsawad *et al.*, 2004). Langedijk *et al.* (1997) have proposed a three-dimensional model for the structure of haemagglutinin/neuraminidase (HN) and haemagglutinin (H) proteins of viruses within this family. This model generated a hypothetical structure for HeV G that closely resembled respiroviruses and rubulaviruses more than morbilliviruses (Yu *et al.*, 1998). We wished to determine whether the location of virus neutralization related amino acid sites in HeV resembled those determined for other *Paramyxovirinae* and how these sites presented within the proposed model. We selected neutralization-escape HeV variants using anti-HeV G monoclonal antibodies (mAbs), determined the location and nature of amino acid substitutions in individual variants and mapped them onto the HeV G globular head model (Yu *et al.*, 1998). Potential spatial and conformational relationships between individual epitopes were investigated by determining the extent of individual mAb binding to and neutralization of, homologous and heterologous variants. These data and information on the relative ability of the mAbs to compete for binding to HeV G, provided support for the proposed structural model and revealed new information about the antigenic relationships between the G proteins of HeV and NiV.

METHODS

Virus propagation and purification. Vero cells were grown in Eagle's minimal essential medium (EMEM) incorporating 10 % fetal calf serum. HeV, originally sourced from a fatal human case (Selvey *et al.*, 1995), was plaque purified then physically purified by sucrose-gradient centrifugation (Hyatt & Selleck, 1996; Wang *et al.*, 1998). Live virus was handled under Bio-Safety level 4 (BSL-4) conditions. For use as inocula and mAb characterization or for genome extraction, the virus was inactivated by gamma irradiation (0·06 MGy) or by treatment with 2 % SDS at 100 °C for 2 min, respectively. An NiV isolate, originally sourced from the Malaysian outbreak (Chua *et al.*, 1999), was grown and inactivated in the same manner.

Antisera. Human and equine anti-HeV antisera were obtained from the 1994 HeV outbreak (Selvey *et al.*, 1995; Murray *et al.*, 1995). Antisera to HeV were also produced in experimentally infected horses and rabbits under BSL-4 conditions. Swine and equine anti-NiV antisera were obtained during the NiV outbreak in 1999 (Chua *et al.*, 1999; Mohd Nor *et al.*, 2000) and flying fox sera possessing antibodies to HeV were collected in Queensland (Halpin *et al.*, 2000). All sera raised to infectious virus were gamma irradiated at 0·06 MGy prior to use.

Serum neutralization test (SNT). As previously described (Crameri *et al.*, 2002), 50 µl aliquots of serially diluted antibody was mixed with an equal volume of EMEM containing 100 $TCID_{50}$ units of HeV and incubated for 30 min at 37 °C. Vero cells were added and the mixture incubated in the wells of a 96-well plate at 37 °C. The cells were monitored for cytopathic effect (CPE) over 5 days. Dilutions were tested in quadruplicate. Neutralization titres were expressed as the reciprocal of the dilution of antibody that completely blocked development of a CPE.

G protein expression. The full-length HeV G gene was isolated by PCR from cDNA synthesized from total genomic RNA using random hexamer primers, and cloned into the pZErO vector (Invitrogen) for sequencing analysis. The gene was then cut out of the pZErO clone by digestion with *Bam*HI (partial) and *Eco*RI, and subcloned into the pFastBac1 vector (Invitrogen) to form the expression plasmid pFB-HeV-G. The gene was then inserted into bacmid DNA using the Bac-to-Bac system (Invitrogen) and the resultant recombinant (HeV-G-Bac) was transfected into *Spodoptera frugiperda* (Sf21) cells using CELLfectin (Invitrogen). A vaccinia recombinant virus that expressed HeV G (VV-326) was also obtained (Stevens, 2001). This construct used the Western Reserve strain of vaccinia virus and the late promoter of the plasmid pMJ602 (Davison & Moss, 1990). For baculovirus production, Sf21 cells were infected with the recombinant virus at an m.o.i. of 1·0 and infected cells were recovered at 48–72 h post-infection (p.i.). Cell pellets were washed twice and resuspended in an equal volume of 0·1 M PBS (pH 7·2). Following three freeze–thaw cycles at −20 °C, the preparation was sonicated on ice (3 × 10 s pulses) in a bath sonicator (Branson Sonifier 250) set at 80 % output. The preparation was centrifuged for 10 min at 3000 ***g*** and the supernatant retained for use as ELISA antigen. For VV-326 virus production, CV-1 cells were infected at an m.o.i. of 5–10 and the cell layer harvested 24–48 h later. Processing of this pellet was as described for the recombinant baculovirus preparation. Recombinant vaccinia virus-produced HeV G was used for both ELISA and mAb production. The level of HeV G expression from each construct was determined by Western blotting and indirect ELISA (I-ELISA) using hyperimmune rabbit antiserum to purified HeV.

mAb production and characterization. Murine mAbs were prepared as previously described (Eaton *et al.*, 1987) with some variations. For the first cell fusion, 20 µg gamma-irradiated, purified HeV in 100 µl PBS was mixed with an equal volume of Montanide ISA50V adjuvant (SEPPIC) and inoculated intraperitoneally into female BALB/c mice older than 10 weeks of age. Mice were further inoculated with 10 µg purified, inactivated virus alone at 2 and 4 weeks p.i. and at 4 days prior to fusion. A second fusion used 10 µg VV-326-expressed HeV G, prepared as described above, for the second and subsequent inoculations. Hybridoma supernatants were screened against both VV-326- and HeV-G-Bac-expressed HeV G in an I-ELISA. Positive supernatants were tested in an SNT and selected neutralizing mAbs were then grown to a high concentration in a bioreactor system (miniPERM classic; Vivascience AG) as previously described (Bruce *et al.*, 2002). Individual mAb isotypes and post-bioreactor concentrations were simultaneously determined using a bead-based isotyping kit (Beadlyte; Upstate) run on a Bio-Plex protein array system (Bio-Rad) as specified by the manufacturers.

Competitive-binding assay. The ability of one mAb to affect the binding of another was measured using an ELISA-based additivity assay as previously described (Friguet *et al.*, 1983; Choumet *et al.*, 1992), with some modifications. Briefly, mAbs were used at concentrations that saturated the binding capacity of a limiting amount of purified virus (Wong *et al.*, 1992). Pairs of mAbs were analysed with the pre-determined saturating concentration of each being maintained in each case. Results were expressed as a percentage inhibition level rather than an additivity index score. The mean percentage level of maximum potential competition between each mAb pair was determined as follows:

$$[1-[(A_{1+2}-A_1)/2A_2+(A_{1+2}-A_2)/2A_1]]\times 100$$

where A_1 and A_2 were the absorbance values obtained for each mAb

alone and A_{1+2} was the value obtained when the same mAbs were added in combination. Inhibition levels in excess of 30 % were regarded as significant.

Variant virus production. HeV was diluted to 5×10^6 $TCID_{50}$ ml^{-1} in EMEM. Aliquots of 100 µl were incubated with an equal volume of undiluted mAb for 30 min at 37 °C, prior to adsorption onto Vero cells grown to 80 % confluency in 25 cm^2 flasks. Following incubation for 30 min at 37 °C, 5 ml of mAb diluted 1/50 in EMEM was added and incubation continued. Where discrete syncytial foci formed (after 3–5 days) and after the subsequent development of a significant CPE, the supernatant was removed and titrated in a plaque assay. Between 4 and 13 plaques were picked for each mAb and the virus in each plaque was designated by the mAb name followed by V1 to V13. Virus from each original plaque was mixed directly with an equal volume of homologous, undiluted mAb and neutralization resistant variants were grown in Vero cells and plaque picked as before. This process was repeated. Individual clones were tested for neutralization resistance to the homologous mAb and stocks prepared by infecting Vero cells at an m.o.i. of 0·01 $TCID_{50}$ per cell in the absence of mAb.

Normalized variant virus-binding assay. Antigen generated by wild-type and selected variant viruses was prepared 24 h after infection of Vero cells in 150 cm^2 flasks at an m.o.i. of 0·01 $TCID_{50}$ per cell. Cells were scraped from the flask, lysed by Dounce homogenization in the presence of 1 % NP40, and the nuclear and cytoskeletal components removed by centrifugation at 500 ***g*** for 15 min. Antigen was inactivated by gamma irradiation and bound to Maxisorp microplates for analysis by I-ELISA. Non-neutralizing, HeV G-specific mAbs were screened for their ability to bind excess amounts of each variant antigen. mAb 30.6 gave equivalent optical density values with all variant preparations and was consequently included in the mAb panel tested against each variant. The optical density of each neutralizing mAb was normalized in each case to the binding level of mAb 30.6 to yield comparative binding data (White, 1994).

Nucleotide sequencing. Purified, gamma-irradiated HeV was subjected to reverse transcription and PCR amplification using the one-step RT-PCR kit (Qiagen). Five sets of primers were designed to amplify overlapping HeV G gene fragments of between 600 and 800 nt each. Amplified DNA fragments were purified using a QIAquick kit (Qiagen), and sequenced twice in each direction using the ABI PRISM BigDye Terminator Cycle Sequencing kit (Applied Biosystems) and the automated DNA sequencer ABI PRISM 377 (Applied Biosystems). Sequence analysis was conducted using the Lasergene software package (DNASTAR).

RESULTS

Isolation and characterization of virus neutralizing mAbs

Five neutralizing mAbs were obtained from a total of 116 that showed significant reaction with HeV G in the I-ELISA. mAbs H1 and H2.1 were derived from the first fusion that used purified virus in all inoculations and mAbs 3A5.D2, 8H4 and 17A5 resulted from the second fusion that used vaccinia-expressed HeV G in all but the primary inoculation. A non-neutralizing HeV G-specific mAb (30.6) was retained for use in the normalized binding ELISA. All six mAbs possessed the IgG1 isotype. The neutralizing mAbs had similar neutralization titres and levels of binding to HeV, except for mAb 17A5, which had a comparatively much reduced neutralization titre (Table 1). None of the mAbs neutralized NiV, yet mAbs H1, H2.1, 8H4 and 17A5 were able to bind NiV at levels significantly less than the homologous reaction. mAbs 30.6 and 3A5.D2 did not bind to NiV. All of the mAbs failed to react with purified HeV or the expressed HeV G preparations in a conventional SDS-PAGE-based Western blot assay (data not shown).

The location of neutralization epitopes and their relationship to a proposed tertiary structure for HeV G

A common structural model for paramyxovirus attachment proteins (Langedijk *et al.*, 1997) that was applied to HeV G by Yu *et al.* (1998) is presented in Fig. 1. Nucleotide and amino acid changes in each of the 29 variants and their homologous mAbs are shown in Table 2. The amino acid changes are also indicated on a linear sequence of the head region of HeV G (aa 183–604) in Fig. 2. Fig. 2 also displays the locations of the four constituent strands of each of the six β-sheets as described in the legend to Fig. 1. The corresponding sequence for NiV G (Harcourt *et al.*, 2000) is also shown (Fig. 2). The mAbs H1 and H2.1 induced amino acid changes (highlighted in red and yellow, respectively) at three identical locations. Within the cluster at aa 183–185 (site I) that adjoined the 'quasi' S4 strand at

Table 1. The ability of selected G protein-specific mAbs to bind and neutralize NiV and HeV

mAb	Concentration* ($mg\ ml^{-1}$)	Virus neutralizing titre (reciprocal end point)		Virus binding (ELISA optical density)	
		HeV	NiV	HeV	NiV
H1	0·29	4096	0	2·15	0·52
H2.1	0·42	4096	0	1·87	0·49
3A5.D2	2·4	8192	0	2·56	0·05
17A5	0·89	256	0	2·11	0·23
8H4	0·67	8192	0	2·62	0·34
30.6	0·16	0	0	1·08	0·07

*Concentrations were adjusted to 50 µg ml^{-1} prior to use in the ELISA-binding assay.

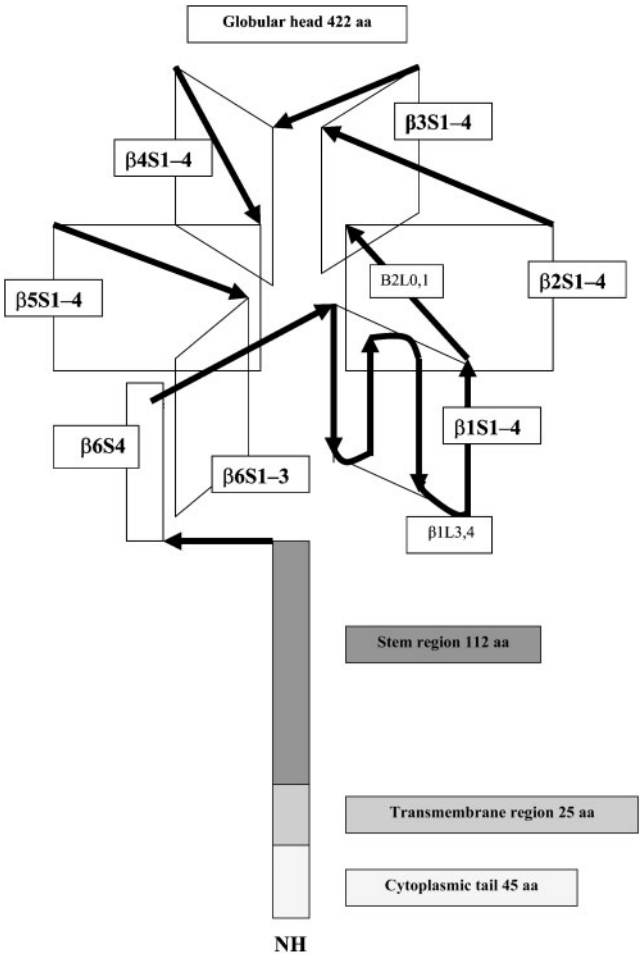

Fig. 1. The proposed model for the structure of HeV G (Langedijk *et al*., 1997; Yu *et al*., 1998), including the tail, transmembrane, stem and globular head regions. The globular head is composed of six folded anti-parallel β-sheets (β1–6) each containing four strands (S1–4), with each β-sheet radiating out from the central axis of the molecule like propeller blades. The S1 strand is closest to the axis and the S4 strand furthest away. Strands within a sheet are connected by loops. Thus, β1L3,4 is the loop linking strands S3 and S4 at the bottom of the first β-sheet. The fourth strand of each sheet is connected across the top of the molecule to the first strand of the next sheet. Thus, β2L0,1 is the loop attaching β-sheets 1 and 2 on the top of the globular head. Eight amino acids (186–193) that follow almost immediately after the protein stem provide a 'quasi' fourth strand (β6S4) adjacent to the three conventional strands (β6S1–3) constituting the β6-sheet. For simplicity of presentation, the four strands have been omitted from each of the remaining sheets.

the bottom of the β6-sheet, at aa 517 (site VII) at the bottom of β5-sheet in the β5L1,2 loop and at aa 570 (site VIII) in loop L1,2 at the bottom of the β6-sheet. The alteration at aa 447 (site VI) (at the end of β4S1 towards the bottom of the β4-sheet), only occurred in a variant selected with H2.1 (Table 2).

Table 2. Sites defining regions of amino acid substitutions in the HeV G protein of mAb-selected neutralization-escape variant viruses

Site	mAb	Variant	Nucleotide substitution	Amino acid substitution
I	H1	H1 V2	547 (G to A)	183 (Gly to Arg)
		H1 V4	547 (G to A)	–
		H1 V5	547 (G to A)	–
		H1 V7	547 (G to A)	–
		H1 V6	548 (G to A)	183 (Gly to Glu)
	H2.1	H2.1 V1	548 (G to A)	–
		H2.1 V4	551 (T to C)	184 (Leu to Pro)
		H2.1 V2	554 (C to A)	185 (Pro to Gln)
		H2.1 V9	554 (C to A)	–
		H2.1 V13	554 (C to A)	–
II	17A5	17A5 V2	573 (G to T)	191 (Gln to His)
		17A5 V3	574 (A to G)	192 (Lys to Glu)
		17A5 V1	583 (T to C)	195 (Ser to Pro)
III	8H4	8H4 V1	865 (G to T)	289 (Asp to Tyr)
		8H4 V3	865 (G to T)	–
		8H4 V5	865 (G to T)	–
		8H4 V6	865 (G to T)	–
		8H4 V10	865 (G to T)	–
IV	8H4	8H4 V2	970 (A to G)	324 (Lys to Glu)
		8H4 V4	970 (A to G)	–
V	3A5.D2	3A5.D2 V1	1154 (T to A)	385 (Ile to Asp)
		3A5.D2 V2	1157 (A to G)	386 (His to Arg)
VI	H2.1	H2.1 V8	1340 (C to T)	447 (Ser to Phe)
VII	H1	H1 V3	1550 (T to C)	517 (Leu to Pro)
	H2.1	H2.1 V3	1550 (T to C)	–
		H2.1 V5	1550 (T to C)	–
VIII	H1	H1 V1	1710 (T to A)	570 (Asn to Lys)
		H1 V8	1710 (T to A)	–
	H2.1	H2.1 V6	1710 (T to A)	–

The S1 strand, or the loop linking the S1 strand to S2, therefore appeared to play a key role in three of four sites (VI, VII and VIII). The structural model places the S1 strands of each of the β-sheets towards the central axis of the molecule. In that location, they may be in sufficient proximity to potentially contribute to a single, discontinuous epitope on the underside of the globular head.

Site III (aa 289) and site IV (aa 324) identified in 8H4 variants (highlighted in pink in Fig. 2) both mapped to the bottom of the β2-sheet, at the end of the S1 and at the start of the S4 strands, respectively. Amino acid 289 was located in the middle of a postulated small loop created by a cysteine bridge joining the top of the β2S1 strand to the base of the β2S2 strand (Yu *et al*., 1998). This may bring aa 289 closer to aa 324. Thus, mAb 8H4 defined a second epitope located on the base of the globular head and on the opposite side to the H1/H2.1 epitope. In support of an association between these epitopes, mAbs 8H4 and H1 also exhibited the most significant level of mutual binding inhibition (91 %) in the competition ELISA (Table 3).

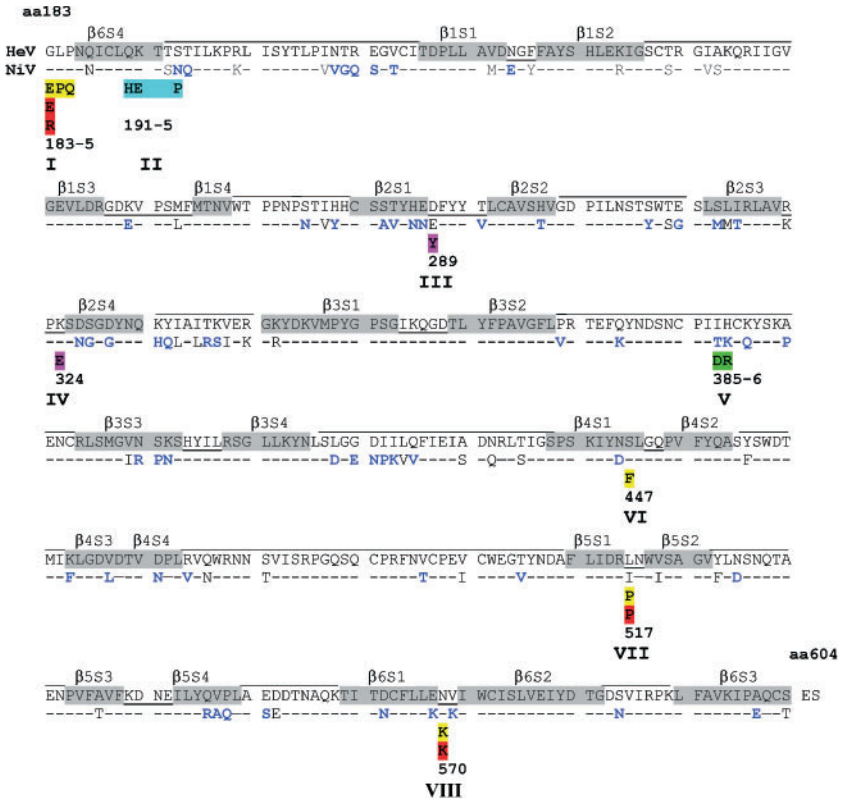

Fig. 2. A linear representation of the sheet and strand structure of HeV G and NiV G, from aa 183–604 and 183–602, respectively, and the location of amino acid alterations found in mAb-selected HeV G mutants. The postulated positions of strands and β-sheets are shaded and lines above and below the amino acid sequence indicate proposed protein loops on the top and bottom of the globular head, respectively (Yu *et al.*, 1998). The positions of amino acid alterations and the mAbs used in their selection are colour coded as follows: red, H1; yellow, H2.1; cyan, 17A5; pink, 8H4; and green, 3A5.D2. The positions of altered amino acid are given below the colour coding. Software-defined, non-conservative amino acid differences between HeV and NiV are highlighted in blue. The eight sites of amino acid change are represented by roman numerals beneath each region of amino acid substitution.

Mutations in 17A5 variants (site II, aa 191–195) and 3A5.D2 variants (site V, aa 385–386) (highlighted in cyan and green, respectively, in Fig. 2) both involved alterations at separate sites on the top of the globular head. For 17A5 variants these were located at the top of the 'quasi' S4 strand in the β6-sheet and for 3A5.D2 variants they were in the centre of the L2,3 loop on top of the β3-sheet. No significant level of inhibition of mutual binding was observed between these two mAbs or between mAb 3A5.D2 and mAb H1 (Table 3). The binding site for mAb 17A5 actually appeared to be in close proximity to the 8H4 and H1/H2.1 binding sites on the base of the globular head (Table 3). In particular, the combination of mAbs 17A5 and 8H4 showed an 86 % level of inhibition of mutual binding to HeV G. mAbs 3A5.D2 and 17A5 showed an insignificant level of mutual binding inhibition (Table 3).

Table 3. Percentage inhibition of mutual binding to HeV G for pairs of mAbs ($mAb_1 + mAb_2$) in a competition ELISA

An inhibition level of >30 % indicated a significant level of mutual inhibition. NT, Not tested.

mAb_1	mAb_2			
	H1	3A5.D2	17A5	8H4
H2.1	89	NT	NT	NT
H1	–	14	68	91
3A5.D2	–	–	26	48
17A5	–	–	–	86

Despite the respective locations of the mAb 3A5.D2 defined epitope (on top of the β3-sheet) and mAb 8H4 defined epitope (at the bottom of the β2-sheet), these mAbs showed an unexpectedly high level of mutual binding inhibition (48 %). However, given that these epitopes resided on adjacent β-sheets, steric hindrance factors or some level of conformational inter-dependency may have prevented optimal binding levels of either or each mAb.

Ability of mAbs to bind and neutralize variants

To determine how particular amino acid substitutions contributed to the presentation of individual mAb-defined epitopes, variants were tested for their ability to bind and be neutralized by the mAb used in their selection and all remaining mAbs (Table 4). All mAbs were compromised in their ability to neutralize variants regardless of the mAb used in their selection. Thus, alterations at any one site induced conformational changes to the globular head of HeV G that influenced the involvement of all the other sites in virus neutralization. Seven variants selected using mAb H1 or H2.1 also displayed an inability to bind to either of these mAbs or be neutralized by mAb H2.1 (mAb H1 was not tested in the SNT) consistent with the hypothesis that mAbs H1 and H2.1 bound the same epitope. All other mAbs bound these variants near, or better than, wild-type levels

Table 4. The ability of selected HeV variant viruses to be bound and neutralized by members of the mAb panel

Reactions between variants and the mAb used in their selection are boxed in each case. Bind., Binding; Neut., neutralizing. NT, Not tested.

Variant		Amino acid substitution	Neutralizing mAb									
			H2.1		H1		17A5		8H4		3A5.D2	
			Bind.*	Neut.†	Bind.	Neut.	Bind.	Neut.	Bind.	Neut.	Bind.	Neut.
H2.1	V1	183	**0·0**	**0·0**	0·0	NT	1·0	0·6	0·9	0·6	0·8	0·6
	V2	185	**0·0**	**0·0**	0·0	NT	1·0	0·6	1·0	0·5	0·8	0·6
	V4	184	**0·0**	**0·0**	0·0	NT	0·9	0·6	1·0	0·5	0·9	0·8
	V8	447	**0·0**	**0·0**	0·0	NT	1·3	0·0	1·3	0·6	0·9	0·6
H1	V1	570	0·0	0·0	**0·0**	**NT**	1·0	0·6	1·2	0·5	1·1	0·6
	V2	183	0·0	0·0	**0·0**	**NT**	1·0	0·4	1·0	0·5	0·9	0·6
	V3	517	0·0	0·0	**0·0**	**NT**	1·0	0·8	1·2	0·6	1·0	0·7
17A5	V1	195	0·6	0·7	0·6	NT	**1·0**	**0·0**	1·1	0·5	0·9	0·8
	V2	191	0·7	0·7	0·8	NT	**0·8**	**0·0**	0·9	0·5	0·9	0·7
	V3	192	0·5	0·7	0·5	NT	**0·8**	**0·0**	0·9	0·5	0·6	0·7
8H4	V1	289	0·6	0·3	0·7	NT	0·2	0·0	**0·0**	**0·0**	0·7	0·5
	V2	324	0·7	0·3	0·8	NT	0·2	0·0	**0·0**	**0·0**	0·7	0·5
3A5.D2	V1	385	0·3	0·0	0·3	NT	1·1	0·8	1·3	0·6	**0·0**	**0·0**
	V2	386	0·4	0·5	0·4	NT	1·2	0·5	0·9	0·5	**0·2**	**0·5**

*Normalized-binding level (see Methods) where a value of 1·0 is equivalent to binding level with wild-type virus. Results are corrected to one decimal place.

†Calculated as $\log_e$ (reciprocal end point titre of mAb with variant)/$\log_e$ (reciprocal end point titre of mAb with wild-type virus) corrected to one decimal place.

which suggested their respective epitopes were distinct from the H1/H2.1 site.

The variants selected by mAbs 8H4, 17A5 and 3A5.D2 were able to bind heterologous mAbs at, or near to, wild-type levels except for mAbs H1 and H2.1. The binding of the latter mAbs to most of the heterologous variants was significantly compromised. The two 3A5 variants showed the least ability to bind mAbs H1 and H2.1 (<50 % wild-type level) and 3A5.D2-V1 was not neutralized by mAb H2.1. Collectively, these data indicated that although the 8H4, 17A5, 3A5.D2 and H1/H1.2 epitopes appeared to be individually distinct, the complex conformation of the latter epitope, comprising regions throughout the length of the head region, still remained sensitive to changes occurring at the other sites. All variants selected with mAbs 3A5.D2 and 8H4 failed to bind (or bound poorly) to their homologous mAb, which indicated the related sites of amino acid substitution (aa 385–386, 289 and 324, respectively) were critical components of the respective mAb-binding sites.

mAb 17A5 bound its three homologous variants at, or near to, wild-type levels. Thus, rather than escaping virus neutralization by impairment of mAb binding, the amino acid changes in these variants apparently affected the way the bound mAb interacted with a critical neutralization site somewhere else on the virus. This mAb showed significantly reduced binding to 8H4 variants and also failed to neutralize them and mAb 8H4 exhibited a similarly reduced ability to neutralize 17A5 variants (Table 4). These observations reaffirmed the suggestion that the epitopes associated with these mAbs existed in close proximity to one another.

Level of amino acid sequence similarity between NiV G and HeV G at the sites of neutralization epitopes located on HeV G

The nucleotide sequences in the immediate region of the identified HeV G neutralization sites were compared to the analogous regions in NiV G (Chua *et al.*, 2002) (Fig. 2). Of the four sites associated with the H1/H2.1 epitope (sites I, VI, VII and VIII) only site VIII showed pronounced differences in the amino acid sequence of each virus immediately adjacent to the site of amino acid substitution (aa 570). These differences alone might have contributed to the much reduced ability of the mAbs H1 and H2.1 to bind NiV, compared with HeV (Table 1). Alternatively, the discontinuous nature of this epitope and the potentially unique overall conformation of NiV G, may result in it being present in an altered state compared with HeV G. Significant differences in sequence similarity were apparent at the mAb 8H4-related regions site III and IV, the mAb 17A5-related site II and the mAb 3A5.D2-related site V and thus provided an explanation for the decreased ability of these mAbs to bind to NiV G (Table 1). In particular, mAb 3A5.D2 failed to bind NiV at all and there were two adjacent amino acid that differed in the HeV and NiV G sequences at site V (-Ile-His- compared with -Thr-Lys-). These 2 aa were critical in the

related HeV variants (Table 4) and most likely represented key residues in this epitope. The lack of analogous residues in NiV G probably prevented the binding of mAb 3A5.D2.

DISCUSSION

Virus neutralizing epitopes on the top of the globular head region of HeV G

Alterations at aa 385 and 386 (site V) identified the mAb 3A5.D2-related epitope. A similar epitope has been defined on the H protein of *Measles virus* (MeV) and *Rinderpest virus* (RPV) (Hu *et al.*, 1993; Ziegler *et al.*, 1996; Moeller *et al.*, 2001; Sugiyama *et al.*, 2002; Putz *et al.*, 2003). This region is cysteine-rich (Fig. 2) and it has been suggested that a cysteine bridge, encompassing 4 aa, exists at this location in MeV, RPV, HeV and NiV (Yu *et al.*, 1998; Harcourt *et al.*, 2000) and may constitute an important structure for antigenic expression (Hu & Norrby, 1994; Ziegler *et al.*, 1996; Putz *et al.*, 2003). A neutralizing epitope has also been reported in a similar region of the HN protein of *Mumps virus* (Cusi *et al.*, 2001). The HeV G structural model predicts that site V is located in the centre of a particularly large loop structure linking S2 and S3 strands in β3-sheet (β3L2,3) (Yu *et al.*, 1998). This region is situated on top of the globular head and is a highly immunogenic region in many *Paramyxoviridae* (Langedijk *et al.*, 1997). It has also been proposed as a potential host cell receptor-binding region (Colman *et al.*, 1993; Langedijk *et al.*, 1997; Iorio *et al.*, 2001; Vongpunsawad *et al.*, 2004).

Amino acid substitutions in 17A5 variants (site II, aa 191–195) mapped to the top of the postulated β6S4-sheet and the β1L0,1 loop. In spite of its unique location, site II related variants resemble their mAb H1/H2.1 and mAb 8H4-selected counterparts in having amino acid changes that appear to influence the conformation of a distal virus neutralization-associated site. Variants selected by mAb 17A5 still bound the homologous mAb and mAb 8H4 at, or near, wild-type level and mAb 3A5.D2 also bound two of the three 17A5 variants at normal level (Table 4). Thus, the reduced ability of mAbs 17A5, 8H4 and 3A5.D2 to neutralize the 17A5 variants would appear to be due to a site II orchestrated conformational alteration that influences virus neutralization more profoundly than mAb binding at specific epitopes.

Separate discontinuous virus neutralization epitopes are on the underside of the globular head region of HeV G

The alignment of amino acid alterations in variants selected by mAbs H1/H2.1 (sites I, VI, VII and VIII) and mAb 8H4 (sites III and IV) with the proposed three-dimensional model for HeV G has identified two discontinuous virus neutralizing epitopes, involving the base of the postulated β-sheets β4–6 and β2, respectively (Table 3, Figs 1 and 2). Discontinuous domains related to host-cell attachment and/or HN activity also occur on the globular head of the attachment proteins of many other *Paramyxoviridae* (van Wyke Coelingh *et al.*, 1987; Makela *et al.*, 1989a, b; Lyn *et al.*, 1991; Iorio *et al.*, 1991, 2001; Ray *et al.*, 1992; Baty & Randall, 1993; Hu *et al.*, 1993; Langedijk *et al.*, 1997; Moeller *et al.*, 2001; Masse *et al.*, 2002, 2004; Vongpunsawad *et al.*, 2004). These though, are frequently located on the top of the globular head once the relevant amino acid locations are integrated into the postulated model (Langedijk *et al.*, 1997; Crennell *et al.*, 2000; Vongpunsawad *et al.*, 2004). However, also according to the model, some point mutations and assumed linear epitopes defined by other paramyxovirus neutralization-escape variant studies include amino acid changes at sites that closely approximate some of the component sites of the H1/H2.1 epitope. A major epitope of RPV mapped to the region aa 587–592 of the attachment protein, within 17 aa of the C terminus of the protein (Sugiyama *et al.*, 2002). This would place it at the bottom of strand β6S4 at a similar location to site I (aa 183–185). An analogous epitope has also been characterized for MeV using synthetic peptides (Makela *et al.*, 1989a, b). The RPV study also identified a mutation at aa 556 that, it was implied, influenced the conformation of the true-binding site of the mAb used in selection of the relevant variant (Sugiyama *et al.*, 2002). This site is analogous to site VIII (aa 570) and is located in the β6L1,2 loop. A substitution at aa 541 on the HN molecule of a variant of *Simian virus 5* also occupied a similar location to site VIII (Baty & Randall, 1993), and a substitution at aa 552 on the H protein was related to neutralization-resistance in MeV (Hu *et al.*, 1993). Thus, HeV resembles other members of the subfamily *Paramyxovirinae* in having critical amino acid sites related to virus neutralization on the underside of the globular head of the attachment protein involving the base of β-sheets 4–6.

Structural relationships between neutralizing epitopes and their potential influence on HeV G cell attachment

The base of the globular head is unlikely to be the location of the host cell receptor, a structure more likely to present on the more accessible upper surface of the protein (Colman *et al.*, 1993; Langedijk *et al.*, 1997; Crennell *et al.*, 2000; Iorio *et al.*, 2001; Masse *et al.*, 2004). However, antibody binding to the underside of the protein head could induce conformational changes to the head region that affects its ability to bind a host cell receptor or facilitate cell fusion (Iorio *et al.*, 1992; Deng *et al.*, 1999; Hu *et al.*, 2004; Masse *et al.*, 2004; Vongpunsawad *et al.*, 2004). Alternatively, a channel or groove may be present through the head that permits access from the top of the protein to regions located deep within the structure. A 'funnel' structure on top of the globular head has in fact been proposed to be associated with neuraminidase (N) activity in paramyxoviruses (Langedijk *et al.*, 1997; Vongpunsawad *et al.*, 2004). A link between the epitopes mapped to the top of the globular head (related to mAbs 3A5.D2 and 17A5) and to the bottom (mAbs H1/H2.1 and 8H4) in this study was implied by the

impaired ability of heterologous mAbs to neutralize H1/H2.1 variants (Table 4). An interaction between the H1/H2.1 and 3A5.D2 sites was particularly indicated by the greatly reduced ability of mAbs H1 and H2 to bind to 3A5.D2 variants. A cross-linkage between one of the three cysteine residues (aa 396) in the loop β3L2,3 and a cysteine residue in the middle of the large loop connecting the top of the β4-sheet to that of the β5-sheet (β4L1,0) has been previously proposed (Langedijk *et al.*, 1997). Thus, the top of the β3-sheet in the L2,3 loop (the postulated site of the 3A5.D2 epitope) could directly influence the underside of the globular head in sheets β4–6, which appears to include the conformation-dependent H1/2.1 epitope. Of further interest was the observation that the H1/H2.1 epitope related site VI (aa 447, postulated to lie on the β4S1 strand near the base of the globular head) is analogous to a region on MeV H (aa 429–438), which has been shown to be associated with binding to the known host cell receptor, signalling lymphocyte activation molecule (SLAM) (Hu *et al.*, 2004). In addition, site VIII (aa 570) maps relatively closely to specific amino acids (546, 548 and 549) recognized to be within a region of MeV H (approx. β5S4 to β6S1 in the postulated model) that has been implicated in haemadsorption and cell receptor (CD46) binding (Masse *et al.*, 2002, 2004). Therefore, similarly to MeV, sites VI and VIII, although associated with the base of the globular head of HeV G, may still have an involvement in receptor binding.

Immunological relationships between HeV and NiV G proteins

The binding of all five mAbs used in this study was significantly inhibited by field-derived human, bat and horse antiserum to HeV and also pig antiserum to NiV, when tested in a competitive ELISA format incorporating expressed HeV G (J. R. White, V. Boyd, G. S. Crameri & C. J. Duch, unpublished results). Considerable cross-neutralization also occurs between these viruses (Harcourt *et al.*, 2000; Wang *et al.*, 2001) and between their G proteins (Bossart *et al.*, 2005) using polyvalent antisera. However, mAbs that neutralized both HeV and NiV were not isolated in this study. Rather, there seemed very little conservation of neutralization epitopes between HeV G and NiV G (Table 1), with only one (HeV1/2.1) exhibiting relatively high levels of conserved amino acid similarity at three of four sites related to this epitope (Fig. 2). Thus, other neutralizing epitopes remain to be identified on HeV G. Alternatively, because the mAbs possessed a reduced affinity for NiV (Table 1), the multi-hit model for virus neutralization (Burton *et al.*, 2001) might explain how individual neutralizing mAbs, each with reduced affinity for a heterologous virus, may still achieve heterologous neutralization when acting together, as would occur in a polyclonal antiserum response.

Structural relationships between henipaviruses and other *Paramyxovirdae*

Despite the proposed folding pattern of the globular head region of HeV G appearing most similar to respiroviruses (Langedijk *et al.*, 1997; Yu *et al.*, 1998; Wang *et al.*, 2001; Eaton *et al.*, 2004), the location of the epitopes described in this study resembled those found on at least two morbilliviruses (Makela *et al.*, 1989a, b; Hu *et al.*, 1993, 2004; Hu & Norrby, 1994; Ziegler *et al.*, 1996; Cusi *et al.*, 2001; Moeller *et al.*, 2001; Sugiyama *et al.*, 2002; Putz *et al.*, 2003; Masse *et al.*, 2002, 2004). Recent publications of revised three-dimensional models for the general structure of the H protein of morbilliviruses (Masse *et al.*, 2004; Vongpunsawad *et al.*, 2004), based upon the known crystal structure of *Newcastle disease virus* HN protein (Crennell *et al.*, 2000), also indicate the similarities between HeV and respiroviruses are less remarkable than previously implied, particularly for sites on the β6-sheet (Langedijk *et al.*, 1997; Masse *et al.*, 2004; Vongpunsawad *et al.*, 2004). Henipaviruses, like morbilliviruses but unlike most other *Paramyxoviridae*, possess no N activity (Murray *et al.*, 1995; Wang *et al.*, 2001) and indeed, some of the virus neutralization related amino acid sites identified in this study appear to be in similar locations to sites implicated in MeV cell receptor binding (Masse *et al.*, 2002, 2004; Hu *et al.*, 2004; Vongpunsawad *et al.*, 2004). It is hoped the data and hypotheses presented in this study will assist with ongoing efforts to characterize further the nature of *Henipavirus* neutralization by host antisera and help to locate the host cell receptor site(s) on HeV G that will ultimately facilitate identification of potential host cell receptor molecules (Bossart *et al.*, 2002; Eaton *et al.*, 2004).

ACKNOWLEDGEMENTS

The authors wish to thank our colleagues Dr Katharine Bossart for her diligent and incisive review of this manuscript and Dr David Boyle for kindly providing the recombinant vaccinia virus VV-326.

REFERENCES

AbuBakar, S., Chang, L. Y., Ali, A. R., Sharifah, S. H., Yusoff, K. & Zamrod, Z. (2004). Isolation and molecular identification of Nipah virus from pigs. *Emerg Infect Dis* **10**, 2228–2230.

Anonymous (2004). *Hendra virus* – Australia. Australian Broadcasting Corporation report, 14 December 2004. The International Society for Infectious Diseases.

Baty, D. U. & Randall, R. E. (1993). Multiple amino acid substitutions in the HN protein of the paramyxovirus, SV5, are selected for in monoclonal antibody resistant mutants. *Arch Virol* **131**, 217–224.

Bossart, K. N., Wang, L.-F., Flora, M. N., Chua, K. B., Lam, S. K., Eaton, B. T. & Broder, C. C. (2002). Membrane fusion tropism and heterotypic functional activities of the Nipah virus and Hendra virus envelope glycoproteins. *J Virol* **76**, 11186–11198.

Bossart, K. N., Crameri, G., Dimitrov, A. S. & 7 other authors (2005). Receptor binding, fusion inhibition, and induction of cross-reactive neutralizing antibodies by a soluble G glycoprotein of Hendra virus. *J Virol* **79**, 6690–6702.

Bruce, M. P., Boyd, V., Duch, C. & White, J. R. (2002). Dialysis-based bioreactor systems for the production of monoclonal antibodies – alternatives to ascites production in mice. *J Immunol Methods* **264**, 59–68.

Burton, D. R., Saphire, E. O. & Parren, P. W. H. I. (2001). A model for neutralization of viruses based on antibody coating of the virion surface. *Curr Top Microbiol Immunol* **260**, 109–143.

Choumet, V., Faure, G., Robbe-Vincent, A., Saliou, B., Mazie, J. C. & Bon, C. (1992). Immunochemical analysis of a snake venom phospholipase A_2 neurotoxin, crotoxin, with monoclonal antibodies. *Mol Immunol* **29**, 871–882.

Chua, K. B. (2003). Nipah virus outbreak in Malaysia. *J Clin Virol* **26**, 265–275.

Chua, K. B., Goh, K. J., Wong, K. T. & 7 other authors (1999). Fatal encephalitis due to Nipah virus among pig-farmers in Malaysia. *Lancet* **354**, 1257–1259.

Chua, K. B., Bellini, W. J., Rota, P. A. & 17 other authors (2000). Nipah virus. A newly emergent deadly paramyxovirus. *Science* **288**, 1433–1435.

Chua, K. B., Koh, C. L., Hooi, P. S., Wee, K. F., Khong, J. H., Chua, B. H., Chan, Y. P., Lim, M. E. & Lam, S. K. (2002). Isolation of Nipah virus from Malaysian island flying-foxes. *Microbes Infect* **4**, 145–151.

Colman, P. M., Hoyne, P. A. & Lawrence, M. C. (1993). Sequence and structure alignment of paramyxovirus hemagglutinin-neuraminidase with influenza virus neuraminidase. *J Virol* **67**, 2972–2980.

Crameri, G., Wang, L.-F., Morrissy, C., White, J. & Eaton, B. T. (2002). A rapid immune plaque assay for the detection of Hendra and Nipah viruses and anti-virus antibodies. *J Virol Methods* **99**, 41–51.

Crennell, S., Takimoto, T., Portner, A. & Taylor, G. (2000). Crystal structure of the multifunctional paramyxovirus hemagglutinin-neuraminidase. *Nat Struct Biol* **7**, 1068–1074.

Cusi, M. G., Fischer, S., Sedlmeier, R., Valassina, M., Valensin, P. E., Donati, M. & Neubert, W. J. (2001). Localization of a new neutralizing epitope on the mumps virus hemagglutinin-neuraminidase protein. *Virus Res* **74**, 133–137.

Davison, A. J. & Moss, B. (1990). New vaccinia virus recombination plasmids incorporating a synthetic late promoter for high level expression of foreign proteins. *Nucleic Acids Res* **18**, 4285–4286.

Deng, R., Wang, Z., Mahon, P. J., Marinello, M., Mirza, A. & Iorio, R. M. (1999). Mutations in the Newcastle disease virus hemagglutinin-neuraminidase protein that interfere with its ability to interact with the homologous F protein in the promotion of fusion. *Virology* **253**, 43–54.

Eaton, B. T., Hyatt, A. D. & White, J. R. (1987). Association of bluetongue virus with the cytoskeleton. *Virology* **157**, 107–116.

Eaton, B. T., Wright, P. J., Wang, L.-F., Sergeyev, O., Michalski, W. P., Bossart, K. N. & Broder, C. C. (2004). Henipaviruses: recent observations on regulation of transcription and the nature of the cell receptor. *Arch Virol Suppl* **18**, 123–131.

Field, H. E., Barratt, P. C., Hughes, R. J., Shield, J. & Sullivan, N. D. (2000). A fatal case of Hendra virus infection in a horse in north Queensland: clinical and epidemiological features. *Aust Vet J* **78**, 279–280.

Friguet, B., Djavadi-Ohaniance, L., Pages, J. & Bussard, A. (1983). A convenient enzyme-linked immunosorbent assay for testing whether monoclonal antibodies recognise the same antigenic site. Applications to hybridomas specific for the β2-subunit of *Escherichia coli* tryptophan synthase. *J Immunol Methods* **60**, 351–358.

Halpin, K., Young, P. L., Field, H. E. & Mackenzie, J. S. (2000). Isolation of Hendra virus from pteropid bats: a natural reservoir of Hendra virus. *J Gen Virol* **81**, 1927–1932.

Harcourt, B. H., Tamin, A., Ksiazek, T. G., Rollin, P. E., Anderson, L. J., Bellini, W. J. & Rota, P. A. (2000). Molecular characterization of Nipah virus, a newly emergent paramyxovirus. *Virology* **271**, 334–349.

Hsu, V. P., Hossain, M. J., Parashar, U. D. & 7 other authors (2004). Nipah virus encephalitis re-emergence, Bangladesh. *Emerg Infect Dis* **10**, 2082–2087.

Hu, A. H. & Norrby, E. (1994). Role of individual cysteine residues in the processing and antigenicity of the measles virus haemagglutinin protein. *J Gen Virol* **75**, 2173–2181.

Hu, A., Sheshberadaran, H., Norrby, E. & Kovamees, J. (1993). Molecular characterization of epitopes on the measles virus hemagglutinin protein. *Virology* **192**, 351–354.

Hu, C. L., Zhang, P., Liu, X., Qi, Y. P., Zou, T. T. & Xu, Q. (2004). Characterization of a region involved in binding of measles virus H protein and its receptor SLAM (CD150). *Biochem Biophys Res Commun* **316**, 698–704.

Hyatt, A. D. & Selleck, P. W. (1996). Ultrastructure of equine morbillivirus. *Virus Res* **43**, 1–15.

Iorio, R. M., Syddall, R. J., Sheehan, J. P., Bratt, M. A., Glickman, R. L. & Riel, A. M. (1991). Neutralization map of the hemagglutinin-neuraminidase glycoprotein of Newcastle disease virus: domains recognised by monoclonal antibodies that prevent receptor recognition. *J Virol* **65**, 4999–5006.

Iorio, R. M., Glickman, R. L. & Sheehan, J. P. (1992). Inhibition of fusion by neutralizing monoclonal antibodies to the haemagglutinin-neuraminidase glycoprotein of Newcastle disease virus. *J Gen Virol* **73**, 1167–1176.

Iorio, R. M., Field, G. M., Sauvron, J. M., Mirza, A. M., Deng, R., Mahon, P. J. & Langedijk, J. P. (2001). Structural and functional relationship between the receptor recognition and neuraminidase activities of the Newcastle disease virus hemagglutinin-neuraminidase protein: receptor recognition is dependent on neuraminidase activity. *J Virol* **75**, 1918–1927.

Johara, M. Y., Field, H., Azmin, M. R. & 8 other authors (2001). Serological evidence of infection with Nipah virus in bats (order Chiroptera) in Peninsular Malaysia. *Emerg Infect Dis* **7**, 439–441.

Langedijk, J. P. M., Daus, F. J. & Van Oirschot, J. T. (1997). Sequence and structure alignment of *Paramyxoviridae* attachment proteins and discovery of enzymatic activity for a morbillivirus hemagglutinin. *J Virol* **71**, 6155–6167.

Lyn, D., Mazanec, M. B., Nedrud, J. G. & Portner, A. (1991). Location of amino acid residues important for the structure and biological function of the haemagglutinin-neuraminidase glycoprotein of Sendai virus by analysis of escape mutants. *J Gen Virol* **72**, 817–824.

Makela, M. J., Salmi, A. A., Norrby, E. & Wild, T. F. (1989a). Monoclonal-antibodies against measles virus haemagglutinin react with synthetic peptides. *Scand J Immunol* **30**, 225–231.

Makela, M. J., Lund, G. A. & Salmi, A. A. (1989b). Antigenicity of the measles virus haemagglutinin studied by using synthetic peptides. *J Gen Virol* **70**, 603–614.

Masse, N., Barrett, T., Muller, C. P., Wild, T. F. & Buckland, R. (2002). Identification of a second major site for CD46 binding in the hemagglutinin protein from a laboratory strain of measles virus (MV): potential consequences for wild-type MV infection. *J Virol* **76**, 13034–130338.

Masse, N., Ainouze, M., Neel, B., Wild, T. F., Buckland, R. & Langerdijk, J. P. M. (2004). Measles virus (MV) hemagglutinin: evidence that attachment sites for MV receptors SLAM and CD46 overlap on the globular head. *J Virol* **78**, 9051–9063.

Middleton, D. J., Westbury, H. A., Morrissy, C. J., van der Heide, B. M., Russell, G. M., Braun, M. A. & Hyatt, A. D. (2002). Experimental Nipah virus infection in pigs and cats. *J Comp Pathol* **126**, 124–136.

Moeller, K., Duffy, I., Duprex, P. & 7 other authors (2001). Recombinant measles viruses expressing altered hemagglutinin (H)

genes: functional separation of mutations determining H antibody escape from neurovirulence. *J Virol* **75**, 7612–7620.

Mohd Nor, N. M., Gan, C. H. & Ong, B. L. (2000). Nipah virus infection of pigs in peninsular Malaysia. *Rev Sci Tech* **19**, 160–165.

Murray, P. K., Selleck, P., Hooper, P. & 8 other authors (1995). A morbillivirus that caused fatal disease in horses and humans. *Science* **268**, 94–97.

Pitt, J. J., Da Silva, E. & Gorman, J. J. (2000). Determination of the disulfide bond arrangement of Newcastle disease virus hemagglutinin neuraminidase. Correlation with a β-sheet propeller structural fold predicted for *Paramyxoviridae* attachment proteins. *J Biol Chem* **275**, 6469–6478.

Putz, M. M., Hoebeke, J., Ammerlaan, W., Schneider, S. & Muller, C. P. (2003). Functional fine-mapping and molecular modeling of a conserved loop epitope of the measles virus hemagglutinin protein. *Eur J Biochem* **270**, 1515–1527.

Ray, R., Duncan, J., Quinn, R. & Matsuoka, Y. (1992). Distinct hemagglutinin and neuraminidase epitopes involved in antigenic variation of recent human parainfluenza virus type 2 isolates. *Virus Res* **24**, 107–113.

Rogers, R. J., Douglas, I. C., Baldock, F. C., Glanville, R. J., Seppanen, K. T., Gleeson, L. J., Selleck, P. W. & Dunn, K. J. (1996). Investigation of a second focus of equine morbillivirus infection in coastal Queensland. *Aust Vet J* **74**, 243–244.

Selvey, L. A., Wells, R. M., McCormack, J. G., Ansford, A. J., Murray, K., Rogers, R. J., Lavercombe, P. S., Selleck, P. & Sheridan, J. W. (1995). Infection of humans and horses by a newly described morbillivirus. *Med J Aust* **162**, 642–645.

Stevens, M. P. (2001). *Biological properties of the Hendra virus envelope proteins*. PhD thesis, Deakin University, Geelong, Australia.

Sugiyama, M., Ito, N., Minamoto, N. & Tanaka, S. (2002). Identification of immunodominant neutralizing epitopes on the hemagglutinin protein of rinderpest virus. *J Virol* **76**, 1691–1696.

Tamin, A., Harcourt, B. H., Ksiazek, T. G., Rollin, P. E., Bellini, W. J. & Rota, P. A. (2002). Functional properties of the fusion and attachment glycoproteins of Nipah virus. *Virology* **296**, 190–200.

van Wyke Coelingh, K. L., Winter, C. C., Jorgensen, E. D. & Murphy, B. R. (1987). Antigenic and structural properties of the hemagglutinin-neuraminidase glycoprotein of human parainfluenza virus type 3: sequence analysis of variants selected with monoclonal antibodies which inhibit infectivity, hemagglutinin and neuraminidase activities. *J Virol* **61**, 1473–1477.

Vongpunsawad, S., Oezgun, N., Braun, W. & Cattaneo, R. (2004). Selectively receptor-blind measles viruses: identification of residues necessary for SLAM- or CD46-induced fusion and their localization on a new hemagglutinin structural model. *J Virol* **78**, 302–313.

Wang, L.-F., Michalski, W. P., Yu, M., Pritchard, L. I., Crameri, G., Shiell, B. & Eaton, B. T. (1998). A novel P/V/C gene in a new member of the *Paramyxoviridae* family, which causes lethal infection in humans, horses, and other animals. *J Virol* **72**, 1482–1490.

Wang, L.-F., Yu, M., Hansson, E., Pritchard, L. I., Michalski, W. P. & Eaton, B. T. (2000). The exceptionally large genome of Hendra virus: support for creation of a new genus within the family *Paramyxoviridae*. *J Virol* **74**, 9972–9979.

Wang, L.-F., Harcourt, B. H., Yu, M., Tamin, A., Rota, P. A., Bellini, W. J. & Eaton, B. T. (2001). Molecular biology of Hendra and Nipah viruses. *Microbes Infect* **3**, 279–287.

White, J. R. (1994). Validation of a quantitative ELISA for comparison of monoclonal antibody affinities for isolates of bluetongue virus. *J Immunol Methods* **177**, 79–88.

Wong, J. P., Fulton, R. E. & Siddiqui, Y. M. (1992). Epitope specificity of monoclonal antibodies against Newcastle disease virus: competitive fluorogenic enzyme-immunoassay. *Hybridoma* **11**, 829–836.

Young, P. L., Halpin, K., Selleck, P. W., Field, H., Gravel, J. L., Kelly, M. A. & MacKenzie, J. S. (1996). Serologic evidence for the presence in Pteropus bats of a paramyxovirus related to equine morbillivirus. *Emerg Infect Dis* **2**, 239–240.

Yu, M., Hansson, E., Langedijk, J. P. M., Eaton, B. T. & Wang, L.-F. (1998). The attachment protein of Hendra virus has high structural similarity but limited primary sequence homology compared with viruses in the genus *Paramyxovirus*. *Virology* **251**, 227–233.

Ziegler, D., Fournier, P., Berbers, G. A. & 7 other authors (1996). Protection against measles virus encephalitis by monoclonal antibodies binding to a cystine loop domain of the H protein mimicked by peptides which are not recognized by maternal antibodies. *J Gen Virol* **77**, 2479–2489.